J. Condensed Matter Nucl. Sci. 19 (2016) 135–144

Research Article

# Effect of Minority Atoms of Binary Ni-based Nano-composites on Anomalous Heat Evolution under Hydrogen Absorption

A. Kitamura*†, A. Takahashi‡, R. Seto and Y. Fujita

*Technova Inc., 1-1 Uchisaiwaicho 1-chome, Chiyoda-ku, Tokyo 100-0011, Japan*

A. Taniike and Y. Furuyama

*Kobe University, Kobe 658-0022, Japan*

**Abstract**

Ni-based binary nano-composite samples supported by mesoporous silica and single-component nickel samples were subjected to hydrogen absorption runs at various temperatures up to 350°C. The former include $Pd_{0.016}Ni_{0.070}/SiO_2$ (PNSII) and $Cu_{0.011}Ni_{0.077}/SiO_2$ (CNS2), and the latter NiO/Ni (NN) and $Ni/SiO_2$ (NS). Only the binary nano-composite samples, PNSII and CNS2, showed excess power reaching 8 W/g-Pd and 1 W/g-Ni with integrated excess energy of 3.8 keV/Pd (6.5 keV/atom-H) and 0.6 keV/Ni (10 keV/atom-H), respectively, in elevated temperature runs, implying a catalytic effect of the minority atoms on the phenomena. These excess heat values were observed after the saturation of H-absorption to metal, which implies a non-chemical source of energy.
 ISSN 2227-3123

*Keywords:* Cu·Ni/$SiO_2$ nano-composite, Excess energy, Hydrogen gas absorption, Oil-flow calorimetry, Mesoporous silica, 10 keV/atom-H

## 1. Introduction

Phenomena of anomalous heat evolution from hydrogen-isotope-loaded metal-oxide samples have been studied using a twin absorption system $A_1A_2$, e.g., [1,2], and a scaled-up system $C_1$ with a ten-times larger reaction chamber equipped with a flow calorimeter employing an oil coolant with a boiling point of 390°C [3–5]. The former was used for experiments at room temperature mainly for Pd-based and Ni-based nano-composite samples supported by or mixed with zirconia to show the effectiveness of metal-oxide nano-particles for the production of anomalously large hydrogen uptake and associated heat. The samples include $Pd/ZrO_2$ (PZ), $Pd_{0.08}Ni_{0.35}/ZrO_2$ (PNZ), $Pd_{0.04}Ni_{0.29}/ZrO_2$ (PNZ2B),

*E-mail: kitamuraakira3@gmail.com
†Also at: Kobe University, 5-1-1 Fukaeminami, Higashinada, Kobe 558-0022, Japan.
‡Also at: Osaka University, 1-1 Yamadaoka, Suita, Osaka 565-0871, Japan.

 ISSN 2227-3123

$Ni/ZrO_2$ (NZ), $Cu_{0.081}Ni_{0.36}/ZrO_2$ (CNZ) and $Cu_{0.21}Ni_{0.21}/ZrO_2$ (CNZIV). The system was also used for samples supported by mesoporous silica (mp-silica), $Pd/SiO_2$ (PS) and $Pd_{0.011}Ni_{0.062}/SiO_2$ (PNS), to reveal the effectiveness of the mp-silica as a substrate for the nanoparticles.

On the other hand, the latter system, $C_1$, was fabricated to make precise measurements at elevated temperatures, mainly for Ni-based binary nano-composite samples, $Cu_{0.02}Ni_{0.083}/SiO_2$ (CNS), $Cu_{0.076}Ni_{0.36}/ZrO_2$ (CNZ4), $Pd_{0.016}Ni_{0.070}/SiO_2$ (PNSII) and $Cu_{0.011}Ni_{0.077}/SiO_2$ (CNS2). References [3–5] describe the results of the absorption runs yielding some excess heat up to 30–100 eV/atom-Ni or 5 W/g-Ni.

The above results have made us infer that surface adatoms of the minor component have a catalytic effect of enabling hydrogen absorption of the host crystalline bulk and release of enhanced anomalous heat. To confirm this point, a single-component sample supported by mp-silica, $Ni/SiO_2$ (NS), has been subjected to the absorption runs. The present paper describes the performance of the NS sample in comparison with those of the binary nano-composite samples [5] to discuss effect of minority atoms of the binary nano-composites on anomalous heat evolution.

## 2. Description of the System

A schematic of the experimental system $C_1$ is shown in Fig. 1. For detailed description of the system including the results of calibration of the flow calorimetry with a flow rate of 10 $cm^3$/min, refer to the previous paper [5]. From

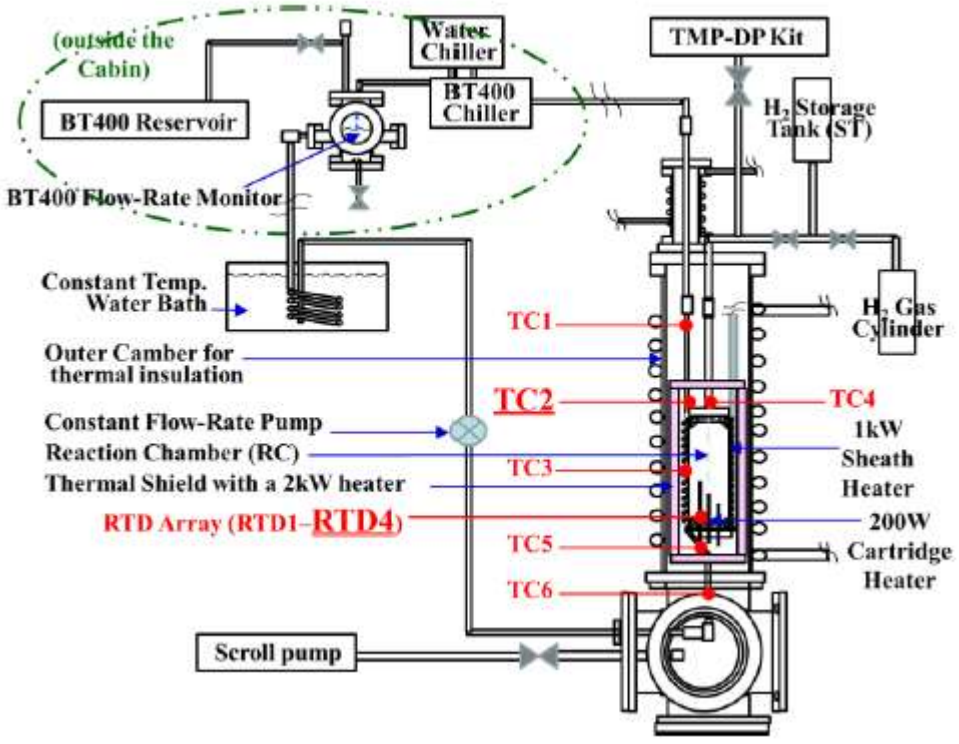


**Figure 1.** Schematic of the $C_1$ absorption system after modification of the flow-rate-monitor and addition of the 200-W cartridge heater inside the reaction chamber.

the calibration runs using an $Al_2O_3$ powder A-12, Showa Denko K.K. [6], the heat conversion coefficient, $dT_{C2}/dW$ = 2.7°C/W or 1.33°C/W, was obtained at room temperature or at the temperature range from 200 to 300°C, respectively. The heat recovery rate was calculated by

$$R_h = F\rho C(T_{C2} - T_{C6})/(W_1 + W_2), \quad (1)$$

where $F$, $\rho$ and $C$ are the flow rate, the mass density and the specific heat capacity, respectively, of the coolant BarrelTherm-400 (BT400), Matsumura Oil Co. Ltd., and $W_1$ and $W_2$ the outer (#1) and the inner (#2) cartridge heater power, respectively. The mean value of $R_h = 0.8$ is a little lower than that in the case of the $C_1$ system before the addition of the heater #2 due to increased loss of heat through the lead wire. The values of $dT_{C2}/dW$ = 2.7°C/W or 1.33°C/W will be used to calculate the excess power observed in room temperature runs or elevated temperature runs, respectively. The calibration run also serves as a control run for foreground runs using the Ni-based samples.

## 3. Hydrogen Absorption Run for Single-component Nickel Sample NS

The single-component nickel nanoparticle samples include the commercially available pure nickel nanoparticle sample, "QSI-Nano Nickel" powder, QuantumSphere Inc. [7], and a home-synthesized nickel nano-particles supported by the mp-silica, which we call the "NS" sample. Performance of the former, which we call the "NN" sample, has been described in [5]. In the present paper, the absorption runs for the NS sample and its performance are described.

The NS sample was synthesized from a nickel chloride solution, according to the recipe provided by Admatechs Inc. [8]. The solution contains the mp-silica powder as a suspended material. After filtration, the mp-silica was annealed at 800°C for 3 h, and milled with a ball mill. Since we prepared sufficient amount of the sample to occupy 500 $cm^3$ volume of the reaction chamber, it was not necessary to add any filler like alumina used in the cases of CNS, CNZ4 and PNSII samples. The 144 g of the sample supporting 16.7 g (0.28 mol) of nickel filled the reaction chamber. Although we have not yet done XRD measurements for this sample, we expect similar results to those for the CNS2 sample described in [5], showing that almost all nickel atoms in the virgin sample are oxidized and perfectly deoxidized during the hydrogen absorption runs. We also expect results of STEM/EDS similar to those for the CNS2 sample described in the next section, showing that nickel nano-particles are trapped in pores of mp-silica. These points would be confirmed by measurements of XRD and STEM/EDS for the NS sample.

Protium (H) absorption runs, H-NS#1 through H-NS#4, were performed after vacuum baking for 45 h at temperatures 230–290°C with the heater power of $(W_1 + W_2)$ = (69+20) W. The temperature history in the H-NS#1 run, e.g., is shown in Fig. 2. Each time the heater power was varied, the phase number is advanced; #1–1 for (0 + 0) W, #1–2 for (10 + 5) W, #1–3 for (20 + 10) W, and so on. In the figure also shown are the pressures at the reaction chamber and at the ST, $P_r$ and $P_s$, respectively, and (H/Ni), the number of H atoms lost from the gas phase relative to the number of nickel atoms, which is calculated from the values of $P_r$ and $P_s$, and volumes of the reaction chamber and the ST with a correction for the temperature based on the Boyle–Charles' law.

The most important variable among the temperatures at TC1 through TC6 and RTD1 through RTD4 is that at TC2, monitoring the oil-outlet temperature $T_{C2}$, while the oil-inlet temperature being monitored by TC6 always remained near room temperature. The TC2 temperature in the H-NS runs, $T_{C2}$(NS), are compared in Fig. 3 with that in the calibration/control run, H-$Al_2O_3$3, $T_{C2}(Al_2O_3)$. As is seen, $T_{C2}$(NS) is somewhat higher than $T_{C2}$,$(Al_2O_3)$ in almost all elevated temperature phases.

In the course of these runs, fluctuation of the flow rate of BT400 was recorded in the flow-rate monitor. A correction for the flow rate fluctuation was made to $T_{C2}(Al_2O_3)$ by adding the deviation $\Delta T_{C2}$ due to the fluctuation $\Delta F$,

$$\Delta T_{C2} = (dT_{C2}/dF)\Delta F = (-\Delta F/F)(W_1 + W_2)(dT_{C2}/dW)\alpha, \quad (2)$$

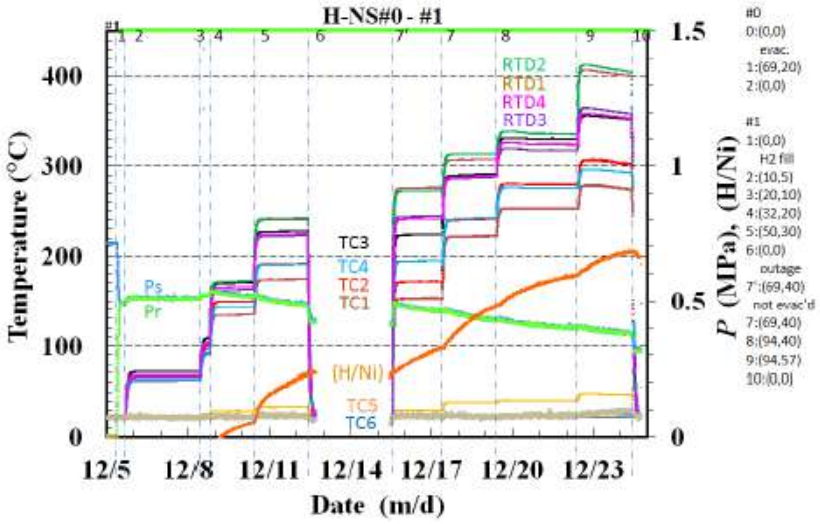


**Figure 2.** Temperature history in the H-NS#1 run.

where $\alpha$ is a fitting parameter. Essentially $\alpha$ has to be 1.0, which is confirmed by deriving Eq. (2) from Eq. (1), or Eq. (1′) below. However, $\alpha$ is determined to be 0.8 from a blank run which is supposed to show no excess heat at all, Ar-CNS2#6 to be described in Section 4. This is consistent with our experience that $(T_{C2}–T_{C6})$ varied with a flow-rate $(F)$ dependence weaker than the linear one, that is $\alpha < 1$ in the modified equation;

$$T_{C2} - T_{C6} = (W_1 + W_2)R_h/(F^{\alpha}\rho C). \tag{1′}$$

The corrected reference temperature, $T_{C2}(Al_2O_3) + \Delta T_{C2}$, is expressed by the blue chain line in Fig. 3. When compared with this corrected reference with the systematic error of about 10°C taken into account, we see no meaningful increase in TC2 temperature $T_{C2}$(NS) in all H-NS runs. We conclude that in the NS powder is induced no anomalous effect, or no excess heat in the temperature range from room temperature to 400°C.

In Fig. 3 the values of (H/Ni) are plotted again. In addition to absorption/adsorption (collectively called 'sorption'), the variable (H/Ni) could involve hydrogen consumption due to oxygen pickup reaction,

$$NiO + H_2 \rightarrow Ni + H_2O + 0.033\ \text{eV}, \tag{3}$$

if the $H_2O$ molecules are either in the liquid phase or in the solid phase due to adsorption. The latter would be possible, if strong adsorption sites happen to be created on the surface of the NS particles or on the mp-silica. The $H_2O$ molecules would remain stuck on the surface throughout the run before the succeeding baking-absorption runs.

The former, i.e., condensation into liquid phase, is also possible in the present system. The virgin sample has 0.28 mol of NiO. If all of NiO molecules are deoxidized, the same amount of $H_2O$ is produced, consuming 0.28 mol of $H_2$, i.e., (H/Ni) $\sim$ 1.0. The $H_2O$ gas would take on a pressure of 1.5 MPa in the part downstream of the SuperNeedle valve including the reaction chamber with a free volume of 420 $cm^3$, if it can remain in the gas phase. However, since the vapor pressure of water at room temperature is 2.3 kPa, almost all of the $H_2O$ molecules will be condensed in the tube outside the reaction chamber at room temperature. The liquid water will be vaporized and removed by subsequent

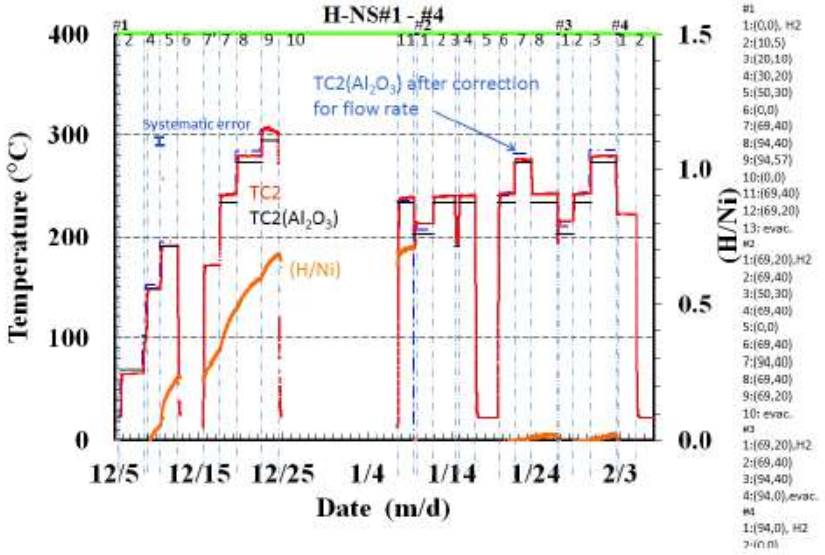


**Figure 3.** Comparison of the temperature at TC2 (*red line*) for NS-sample runs, H-NS/$Al_2O_3$, with that for TC2($Al_2O_3$) in the calibration/control run (*black line*), H-$Al_2O_3$3, and with the TC2($Al_2O_3$) corrected for the flow rate fluctuation *(blue chain line)* to see nonexistence of excess temperature in the H-NS/$Al_2O_3$ runs. Heater powers ($W_1$,$W_2$) in W are indicated on the right. "H2" means $H_2$ gas fill, and "evac." means evacuation.

evacuation prior to the next run. The value of (H/Ni) observed at the final phase before re-baking, #1-12, is 0.7. Then about 1/4 of NiO might have been emitted directly and exhausted during the rebaking phase #1-13.

We observe very small values of (H/Ni) in the succeeding runs, #2, #3 and #4. This means that little reaction (absorption/adsorption) takes place on the single-component nickel nanoparticles supported by the mp-silica at temperatures from room temperature up to 400°C. This is in contrast to the nickel composite samples described in the following section.

## 4. Brief Description of Performance of the CNS2 Sample

The hydrogen absorption runs for the binary nano-composite samples supported by mp-silica have been presented in detail in [3] for the CNS sample and [5] for the PNSII and CNS2 samples. Here results of STEM/EDS characterization and deuterium and argon exposure runs for the CNS2, D-CNS2#5 and Ar-CNS2#6, are described, while the results of the hydrogen absorption runs of the CNS2 samples are only briefly mentioned for comparison. For the detailed description of PNSII and CNS2 samples including XRD characterization, refer to [5].

The 160-g CNS2 sample synthesized in our laboratory with a composition of $Cu_{0.011}Ni_{0.077}/SiO_2$, containing 12 g (0.21 mol) of nickel and 1.9 g (0.03 mol) of copper, occupied the 500 $cm^3$ volume of the reaction chamber, leaving no void to be filled with $Al_2O_3$ powder. A STEM/EDS photo is shown in Fig. 4. It appears that nickel and copper atoms are included in the same pores of the mp-silica with a density ratio approximately equal to the mixing ratio, and diameter of 5–20 nm.

The D and Ar absorption runs, D-CNS2#5 and Ar-CNS2#6, were performed after vacuum baking at temperatures higher than 240°C similarly to other runs. The temperature evolution (the red line) compared with that in the calibra-

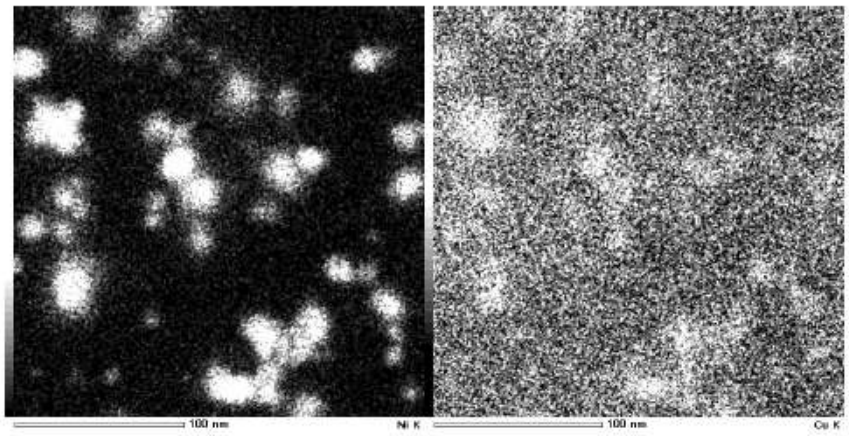


**Figure 4.** STEM/EDS photo of the CNS2 sample showing Cu/Ni particles confined in the nano-pores.

tion/control run H-$Al_2O_3$3 (*the black line*) and the corrected one for flow rate (the blue chain line) is shown in Fig. 5 together with (H/Ni) (*orange line*). Here it is assumed that the Cu atoms are acting as a catalyst for D absorption of nickel lattice, and do not form a lattice to absorb themselves. The correction is based on Eq. (2), with the fitting parameter $\alpha = 0.8$ determined so as to best fit the observed temperature in the Ar-CNS2#6-2 phase, which is supposed to show no excess heat.

This selection gives also null excess in the deuterium absorption run D-CNS2#5, i.e., the differences between

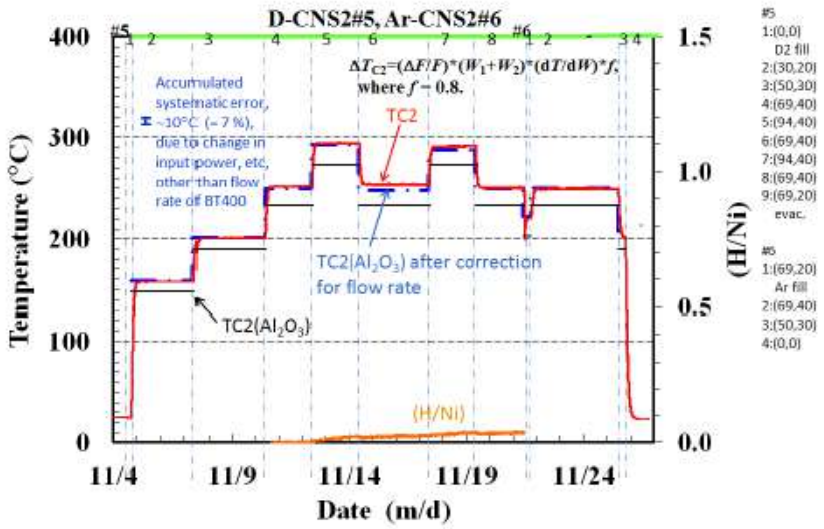


**Figure 5.** Evolution of the temperature at TC2 in the D-CNS2#5 and Ar-CNS2#6 runs compared with that in the calibration/control run H-$Al_2O_3$3. The corrected reference temperature TC2($Al_2O_3$) is calculated by adding $\Delta T_{C2}$ due to deviation of the flow rate of BT400 to the latter.

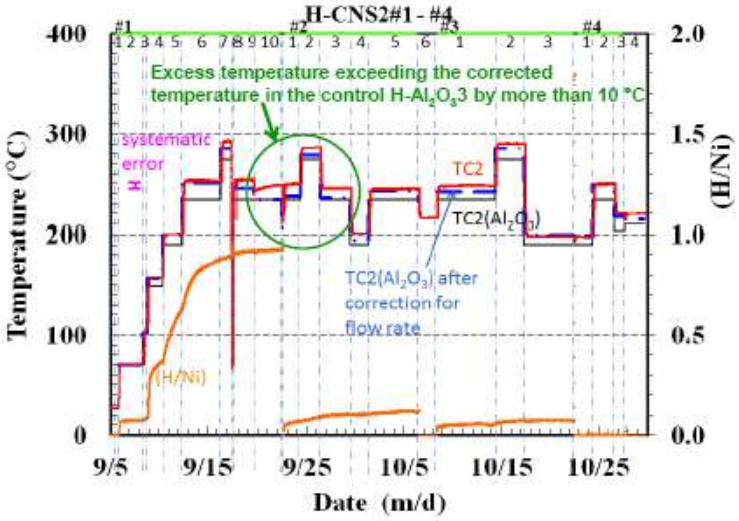


**Figure 6.** An example of the excess heat runs: evolution of the temperature at TC2 in the H-CNS2 runs compared with that in the calibration/control run H-$Al_2O_3$3. Heater powers ($W_1$,$W_2$) in W are: **#1**-1; (0,0) $H_2$ fill, -2;(10,5), -3;(20,10), -4;(30,20), -5;(50,30), -6;(69,40), -7; (94,40), -8;(0,0), -9;(69,40), -10;(69,40) flow rate readjusted, -11;(69,20) evac.; **#2**-1;(69,40) $H_2$ fill, -2;(94,40), -3;(69,40), -4;(50,30), -5;(69,40), -6; (69,20) evac.; **#3**-1;(69,40) $H_2$ fill, -2;(94,40), -3;(50,30), -4;evac.; **#4**-1; (50,30) $H_2$ fill (0.095 MPa), -2;(69,40), -3;(69,20), -4;(69,20) evac.

TC2 and the corrected TC2($Al_2O_3$) are smaller than the systematic error in all phases. This means that the excess heat phenomenon could be isotope dependent in the case of nickel, since the excess heat was clearly observed in H-CNS2#1 through #4 runs. This is consistent with the common belief that nickel works with hydrogen, but not with deuterium. To confirm this point, the temperature evolution in the runs is re-presented in Fig. 6.

In most phases of a variety of the input power, the measured TC2 temperature agrees with the corrected control temperatures (blue chain line) within the systematic error of 10°C, which is comprised of estimated uncertainties in applied heater voltages, location of the thermocouples, and the position / distribution of the heat sources. However, during the period from the phase #1-9 through #2-3, substantial increase beyond the error range is observed. After this period, the excess temperature shows a decline below the systematic error to become null in the phase #3-3 and later.

During this period the maximum excess temperature corresponds to the excess power of 10 W, or 0.8 W/g-Ni, over the input power of 109–134 W. The phase-averaged sorption energy, $\eta_{\mathrm{av},i}$ (eV/atom-H), and the total excess energy per unit absorbent atom, $E_{\mathrm{a,ex}}$ (eV/atom-Ni), are calculated with the following:

$$\eta_{\mathrm{av},i} = \frac{\int_{t-T_i}^{t} W_{\mathrm{a,ex}}\,\mathrm{d}t}{L\,(t) - L\,(t-T_i)}, \tag{4}$$

$$E_{\mathrm{a,ex}} = \int_{0}^{t} W_{\mathrm{a,ex}}\,\mathrm{d}t, \tag{5}$$

where $W_{\mathrm{a,ex}}$ is the specific excess energy (eV/atom-Ni),$L \equiv$ (H/Ni) is the time-dependent loading ratio, and $T_i$ is the period of the phase $i$. They are plotted at the end of each phase in Fig. 7.

The maximum values are $\eta_{\mathrm{av,max}}$ = 1.5 × $10^4$ eV/atom-H and $E_{\mathrm{a,ex}}$ = 3.8 × $10^2$ eV/atom-Ni. The former and the latter are more than three orders of magnitude and two orders of magnitude, respectively, larger than the largest

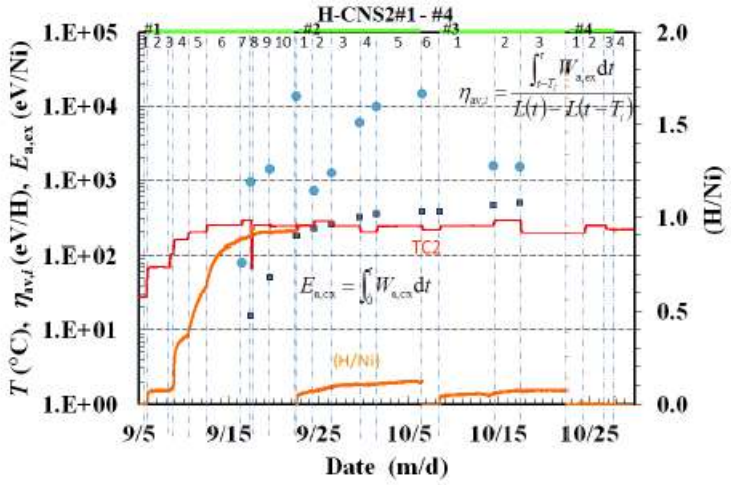


**Figure 7.** Excess energy per H atom, $\eta_{\mathrm{av},i}$ (●), and the integrated excess per nickel atom, $E_{\mathrm{a,ex}}$ (■), both plotted at the end of each phase.

possible value of the conventional chemical reaction energy (which is a few eV/atom). It should be emphasized here that the excess heat emerges in the phases with the loading ratio (H/Ni) approaching saturation and changing only slightly. Especially, $\eta_{\mathrm{av,max}}$ values are estimated by assuming that the small change of the H/Ni ratio contributed totally to the excess heat reaction. However, we do not know what portion of this change of hydrogen transfer was responsible

**Table 1.** Comparison of the samples in regard to excess heat.

| | Sample name | NN/$Al_2O_3$ | NS | PNSII/$Al_2O_3$ | CNS2 |
|---|---|---|---|---|---|
| | M | Ni | Ni | Pd (Pd·Ni) | Ni |
| Transient phase at room temperature in #1 run | *Loading* ratio (H/M) | 0.02 | $\sim 0$ | 3.2 | $\sim 0$ |
| | Specific power (W/g-M) | 0.26 | $\sim 0$ | 3.9 | $\sim 0$ |
| | Sorption energy (eV/atom-M) | 0.17 | $\sim 0$ | 3.0 | $\sim 0$ |
| Transient phase at room temperature in #2 or later | Loading ratio (H/M) | $< 0.02$ | – | 0.87–1.0 | – |
| | Specific power (W/g-M) | $< 0.004$ | – | 0.35–0.43 | – |
| | Sorption energy (eV/atom-M) | $< 0.003$ | – | 0.21–0.19 | – |
| Saturation phase at *elevated temperature* | *Loading* ratio (H/M) in #1 run | 0.23 | $> 0.73$ | 7.6 (1.4) | 0.9 |
| | Loading ratio (H/M) in #2 or later | 0.06 | 0.02 | 2.0–2.5 (0.4) | 0.12–0.08 |
| | Max. excess power (W) | $\sim 0$ | $\sim 0$ | 11 – 8 | 10 |
| | Max. specific excess power $W_{\mathrm{a,ex}}$ (W/g-M) | $\sim 0$ | $\sim 0$ | 7.9–5.9 (2.0) | 0.8 |
| | Specific excess energy $E_{\mathrm{a,ex}}$ (keV/atom-M) | $\sim 0$ | $\sim 0$ | 3.8 (0.68) | 0.38 |
| | Phase-averaged sorption Energy $\eta_{\mathrm{av},i}$ (keV/atom-H) | $\sim 0$ | $\sim 0$ | 2.2–6.5 | 15 |

* 'Loading' in #1 runs includes hydrogen atoms spent for deoxidation of PdO or NiO.
** 'H' stands for either H or D, and 'M' stands for either nickel or palladium.

for the excess energy. The portion may be much smaller. These points make us infer that the excess energy may be of nuclear reaction origin.

## 5. Summary and Concluding Remarks

Another Ni-based nano-composite sample, PNSII, and another single-component nickel sample, NN, were also subjected to hydrogen isotope absorption tests using the same system, and described in detail in [5]. A comparison of the performances of the samples including these two is shown in Table 1. The NN and NS samples showed little heat evolution with no anomaly. At room temperature only the PNSII sample containing palladium absorbed substantial amount of hydrogen with positive heat evolution. The virgin PNSII sample exposed to $D_2$ gas at room temperature showed evolution of heat much larger than the energies emerging from the bulk sorption in addition to oxygen pickup reactions, while in the #2 and later runs the loading ratio and the heat evolution had the values a little larger than or nearly equal to the values characteristic of the bulk palladium sample.

At elevated temperatures both in the PNSII runs and the H-CNS2 runs, excess power was observed in time intervals where the (H/M) ratios varied very slowly, while little excess power was recorded in the phases with rapidly increasing (H/M) in the #1 runs. It appears that the anomalous excess heat at elevated temperatures has some origins other than chemical energy of H-absorption/adsorption. Anyway, it is emphasized that only the binary nano-composite samples showed the excess heat at elevated temperatures. This suggests that the anomalous heat evolution is caused by some catalytic effect of minority atoms, probably the ones making up the conditioned near-surface sites.

Finally, we have to mention that any noticeable change both in the $\gamma$-ray and the neutron counting rates was not

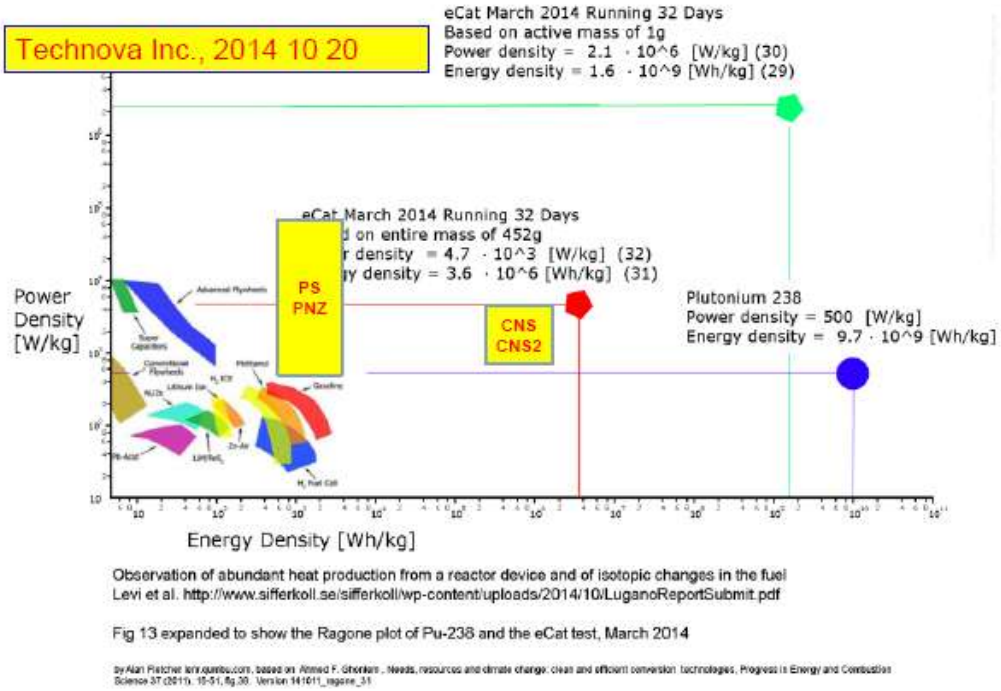


**Figure 8.** Extended Ragone plot. The data from Kobe University–Technova group are added to the original [9].

coincident with the excess power evolution. The range of the specific excess power and the specific excess energy obtained in our laboratory so far are shown in Fig. 8, the extended Ragone plot originally presented in Ref. [9], where the power density vs the energy density obtained by various energy sources are plotted. The sources include the $^{238}$Pu battery and 'eCat' device in addition to conventional ones such as gasoline, $H_2$ fuel cells, Li-ion batteries, advanced flywheels, etc. It is obvious that the present device of ours as well as the 'eCat' has the parameters far superior to conventional energy sources. The energy density of the CNS and CNSII sample runs is as high as 1000 times that of gasoline. Thus, the present apparatus could hopefully be used as a distributed high-energy-density source without hard radiation or radioactive waste.

## Acknowledgement

The authors thank Mr. S. Nagai, Kobe University, for his help in performing the STEM/EDS analysis.

## References

[1] Akira Kitamura, Takayoshi Nohmi, Yu Sasaki, Akira Taniike, Akito Takahashi, Reiko Seto and Yushi Fujita, *Phys. Lett. A* **373** (2009) 3109–3112.
[2] A. Kitamura, Y. Miyoshi, H. Sakoh, A. Taniike, A. Takahashi, R. Seto and Y. Fujita, *J. Condensed Matter Nucl. Sci*. **5** (2011) 42–51.
[3] A. Kitamura, A. Takahashi, R. Seto, Y. Fujita, A. Taniike and Y. Furuyama, *J. Condensed Matter Nucl. Sci*. **15** (2015) 231–239.
[4] A. Kitamura, A. Takahashi, R. Seto, Y. Fujita, A. Taniike and Y. Furuyama, *Proc. JCF14* (2014) 1–13.
[5] A. Kitamura, A. Takahashi, R. Seto, Y. Fujita, A. Taniike and Y. Furuyama, *Proc. JCF15* (2015) 1–19.
[6] http://www.sdk.co.jp/english/products/140/142/2046.html.
[7] http://qsinano.com/wp-content/uploads/2014/05/qsi_nano_nickel_ni_5_oct_09.pdf.
[8] Y. Ookawauti; Private communication.
[9] http://www.networkworld.com/article/2824558/.